Opt Quant Electron (2012) 43:83–90
DOI 10.1007/s11082-011-9505-4

High resolution spectral-domain optical coherence tomography using a thermal light source

Yu-Wei Qin · Hong Zhao · Zhong-Qin Zhuang · Lu Zhang

Received: 3 March 2011 / Accepted: 5 November 2011 / Published online: 22 November 2011

Abstract A high resolution spectral-domain optical coherence tomography (SD-OCT) system based on a thermal light source was presented. A novel normalized method was introduced to remove the background noise and the DC noise of the interference spectrum. A Gaussian spectral calibration procedure was performed to improve axial resolution and image quality before reconstructing OCT image. With the proposed method, the quality of the obtained images was greatly improved. Two-dimensional (2D) cross-sectional images with axial resolution of 1.2 μm were obtained. Furthermore, the film thickness of single-layer film sample was obtained. The experimental result demonstrates the SD-OCT system has potential for film thickness measurement and surface topography.

Keywords Optical coherence tomography · Low-coherence · Thermal light source · Gaussian spectral calibration

1 Introduction

Optical coherence tomography (OCT) is an important imaging technique that can provide non-invasive, non-contact, cross-sectional image of biological tissue and other materials with high resolution (Huang et al. 1991). Since a first two-dimensional cross-sectional image of a human eye fundus contour along a horizontal meridian was presented at the ICO-15 SAT conference in 1990 (Fercher 1990), OCT has been widely used for monitoring and measuring in many fields, such as medical diagnostics and semiconductor material (Bouma et al. 2002; Anna et al. 2009; Brezinski and Fujimoto 1999; Dubey et al. 2007; Drexler and Fujimoto 2008). There are two types of OCT system, time domain OCT (TD-OCT) and

Y.-W. Qin · H. Zhao · Z.-Q. Zhuang · L. Zhang
State Key Laboratory for Manufacturing Systems Engineering, Xi'an Jiaotong University, Xi'an 710049, China

Y.-W. Qin (✉)
School of Physics and Electrical Engineering, Weinan Teachers University, Weinan 714000, China
e-mail: qinyuweimail@gmail.com

Fourier domain OCT (FD-OCT) (Chang et al. 2009). TD-OCT has been proven to be a valid imaging technique for biological tissue during the past years, but the two-dimensional mechanical scanning limits the image acquiring speed. Comparing to TD-OCT, the significant advantages of FD-OCT lies in the higher sensitivity and signal-to-noise ratio (Choma et al. 2003; De Boer et al. 2003). In FD-OCT, the depth information is extracted from the interference spectrum signal of the sample (Chang et al. 2009; Fercher et al. 2003). Because FD-OCT do not contain mechanical axial scan (A-scan) device, its image acquiring speed is higher than TD-OCT. FD-OCT can be further divided into two types, spectral-domain OCT (SD-OCT) and swept-source OCT (SS-OCT) (Fercher et al. 2003; Yun et al. 2003). SD-OCT do not require a scanning delay line, it extracts all interference spectrum signals encoded in frequency in one shot simultaneously. The signals are collected in series from the linear CCD of the spectrometer (Wojtkowski et al. 2002). Depth information of the measured Sample is retrieved via an inverse Fourier transform of spectral interferograms (Fercher et al. 1995). Two-dimensional (2D) cross-sectional and three-dimensional (3D) topography image can be obtained by transversal scanning (B-scan) with this technique.

Generally, low-coherence light sources widely used in SD-OCT were supercontinuum laser and superluminescent diode (SLD), but thermal light source was seldom used. Thermal light source is appropriate for SD-OCT system because of the short coherence length (Fercher et al. 2003, 2000). In this paper, a high resolution SD-OCT technique based on thermal light source with Gaussian spectral calibration is introduced.

2 Principle

The principle of SD-OCT technique is based on low-coherence interferometry (Chang et al. 2009). It relies on scattering potential theory that scattering potential $F_S(z)$ determined by axial microstructure information of the sample can be obtained via an inverse Fourier transform of the scattered light field intensity $E_S(P, k)$ (Fercher et al. 1995).

$$F_S(z) \propto FT^{-1}\{E_S(P, k)\} \tag{1}$$

Where z is axial position, k is the wave number, $E_S(P, k)$ is the amplitude of scattered light field at the detected point p of the sample. Based on the principle of SD-OCT, the interference spectrum signal is

$$I_S(k) \propto S(k)\left\{1 + 2\int_0^\infty F_S(z)\cos(2knz)dz + \int_0^\infty\int_0^\infty F_S(z)F_S(z')\exp[i2kn(z-z')]dzdz'\right\} \tag{2}$$

Where $I_S(k)$ is the interference spectrum signal, $S(k)$ is the spectrum intensity of the light, $F_S(z)$ is the scattering potential of the sample. The first term is the DC noise making the image obscure. The second term is cross-correlation, containing the depth information of the sample. The third term is the auto-correlation which results from the interference signal of the scattering light from different depth of the sample. Compared to the interference signal that the scattering light from the sample interfered with the reflecting light from the reference mirror, the auto-correlation signal is small. It can be ignored because the scattering light is weak in the inner of the sample. From Eq. (2), we can see the interference spectrum signal is a cosine-modulated signal and a periodic modulation signal. Depth information of the sample is retrieved from the second term via an inverse Fourier transform. Before inverse

Fourier transform, interference spectrum signal $I_S(\lambda)$ detected by spectrometer needs to be transformed from λ domain into linear k domain using a cubic spline interpolation method (Chang et al. 2009).

Assuming the low-coherence light source is Gaussian distribution and ignoring dispersion and absorption, the axial resolution of SD-OCT is given by (Fercher et al. 2003).

$$\delta z = l_C/2 = (2\ln 2/\pi)\lambda_0^2/\Delta\lambda \tag{3}$$

where l_C is the coherence length, λ_0 is the central length, and $\Delta\lambda$ is the full width at half maximum (FWHM) spectral bandwidth. According to Eq. (3), the axial resolution of the SD-OCT system is mainly determined by the central wavelength, the spectral bandwidth and the spectral shape of the light source. It is essential for the SD-OCT system to use a low-coherence light source having a broad spectral bandwidth and a Gaussian spectral distribution to achieve higher axial resolution. Tungsten halogen lamp as a type of thermal light source has proven to be an appropriate light source for high resolution OCT system (Fercher et al. 2000; Chang et al. 2009).

3 Experiment setup and result

The SD-OCT system was mainly composed of a fiber Michelson interferometer, a thermal light source and a spectrometer as is shown in Fig. 1.

The incident light originating from tungsten halogen lamp is split into two partially coherent beams by 2×2 fiber coupler (splitting ratio 50:50), the reference beam and the sample beam. The sample beam penetrates into the sample along the axial direction and the reference beam is collimated to the reference mirror. The scattered light from the sample carrying the information of the internal microstructure can be considered as the superposition of quasi-monochromatic light. It interfered with the light of same composition reflected from the reference mirror. The interference spectrum signal was recorded by the spectrometer with the integration time was 1 ms per A-scan. It means the A-scan rate was 1000 scans per second in this system. The motion table was used to perform transversal scanning to get two-dimensional cross-sectional and three-dimensional image. The microscopic objective lens was used to get higher transversal resolution (Fercher et al. 2003). The thermal light source in the system was a tungsten halogen lamp (DT-1000, Ocean Optics) having a Gaussian-like spectral shape. Its spectrum measured by spectrometer was shown in Fig. 2. We can see the spectrum curve was not perfectly Gaussian distribution, therefore, the axial resolution of the system and the imaging quality would be decreased (Fercher et al. 2003; Tsai et al. 2008).

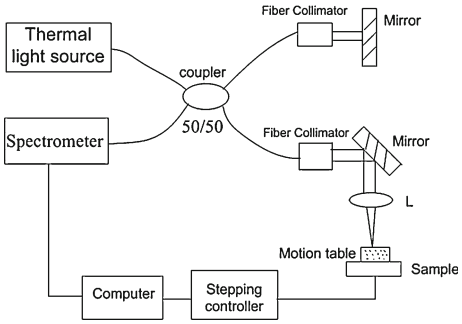

Fig. 1 Schematic of SD-OCT system based on thermal light

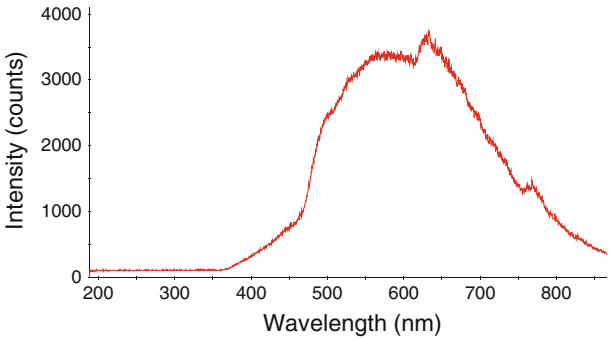

Fig. 2 The spectrum of the tungsten halogen lamp

The central wavelength λ_0 and the full width at half maximum (FWHM) $\Delta\lambda$ of the tungsten halogen lamp was 650 and 225 nm respectively. According to Eq. (3), the theoretical axial resolution of the system was about 0.83 μm. In fact, the actual axial resolution was worse than theoretical value affected by the actual spectrum shape, system noise and other facts (Wojtkowski et al. 2004; Dubey et al. 2008).

In order to remove the DC noise and the background noise, a normalized procedure was introduced in the paper. Assuming a normalized function $T(k)$ can be expressed as follows:

$$T(k) = [I_S(k) - I_D(k)]/[I_R(k) - I_D(k)] \tag{4}$$

where $I_S(k)$ is the interference spectrum, $I_D(k)$ is the spectrum intensity when the sample arm is interrupted. $I_R(k)$ is the spectrum intensity when the sample is replaced with a mirror. Therefore, the normalized interference spectrum $T(k)$can be expressed by

$$T(k) \propto \int_0^\infty F_S(z)\cos(2knz)dz \tag{5}$$

The inverse Fourier transform of $T(k)$ is:

$$FT^{-1}\{T(k)\} \propto [F_S(z) + F_S^*(-z)] \tag{6}$$

From Eq. (6), we can see the DC noise is removed successfully. Meanwhile, the background noise is removed. Because there is no mechanical A-scan device in FD-OCT and interference spectrum is acquired in one shot simultaneously from spectrometer, we only need measure $I_D(k)$ and $I_R(k)$ once in every measurement. Instead of replacing the source with a light source of Gaussian distribution, a simple Gaussian spectral calibration procedure was performed on the normalized interference spectrum to improve axial resolution and the image quality of the OCT system. The normalized interference spectrum $T(k)$ was multiplied by a Gaussian function to get the ideal $I_S(k)$ with a Gaussian light source.

$$I_S(k) = S_G(k)T(k) \propto S_G(k)\int_0^\infty F_S(z)\cos(2knz)dz \tag{7}$$

Then the inverse Fourier transform of $I_S(k)$ is:

$$FT^{-1}\{I_S(k)\} \propto FT^{-1}[S_G(k)] \otimes \hat{F}_S(z) \tag{8}$$

where $\hat{F}_S(z) = F_S(z) + F_S^*(-z)$, $S_G(\lambda) = \frac{2\sqrt{\ln 2/\pi}}{\Delta\lambda} \exp\left\{-4\ln 2\left(\frac{\lambda-\lambda_0}{\Delta\lambda}\right)^2\right\}$

In thin samples, the mirror component $F_S^*(-z)$ can be simply eliminated by introducing additional light path difference into the Michelson interferometer (Targowski et al. 2003), therefore, we can obtain the scattering potential of the sample from Eq. (8). Compared to other Gaussian calibrations approaches (Dubey et al. 2008; Lee and Kim 2008), the proposed approach only relies on the normalization interference spectrum by simple mathematical operations requiring only subtraction and division. Furthermore, the proposed approach can remove the DC noise and the background noise of the image. It doesn't need other sophisticated devices and replace the source with a light source of Gaussian distribution. The processing algorithm is very simple. In order to obtain the axial resolution of the SD-OCT system, a mirror with the same reflectance as the reference mirror was used to calculate the point spread function of the interferometer. The actual axial resolution of the SD-OCT system was 1.5 μm. After spectral calibration procedure, the central wavelength is 670 nm, the full width at half maximum (FWHM) is 165 nm, the actual axial resolution of the SD-OCT system was 1.2 μm as is shown in Fig. 3.

Two samples were used in the experiment, one was a single-layer film coated on glass substrate with the thickness of 18 μm, and the other was a vacuum coating mirror. Figure 4 shows the one-dimensional depth (A-scan) image of the film sample. It also represents the normalized scattering potential of the sample after an inverse Fourier transform of the interference spectrum. From Fig. 4, we can see there are four peaks in the images. Peak 1 and Peak 3 represent the DC noise and the film surface respectively. Peak 2 and Peak 4 represent the boundary between the film and the glass substrate. Before the normalized procedure and the Gaussian spectrum procedure, Peak 2 is small as is shown in Fig. 4a. It will result in the decrease of the signal-to-noise and the image clarity. After the procedures, the DC noise and the background noise are removed and peak 4 is sharper than before as is shown in Fig. 4b. From the position of the two prominent peaks in Fig. 4b, we can see the film thickness is about 16.8 μm.

Figure 5 shows the two-dimensional cross-sectional image of the film. The light line in the image represents the boundary between the film and the glass substrate. Its position corresponds to the position of Peak 4 along depth (A-scan) direction. Before the normalized

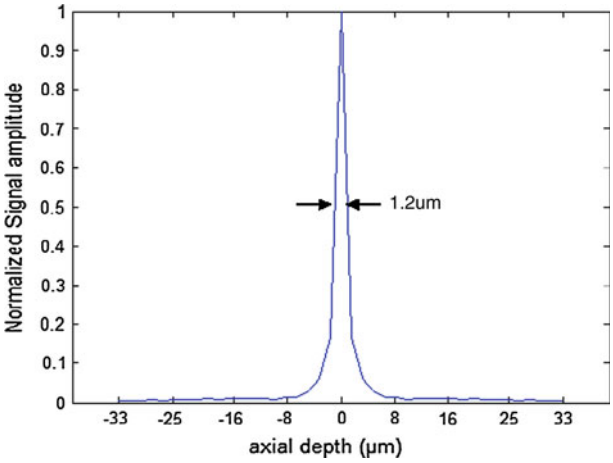

Fig. 3 The point spread function of the SD-OCT system

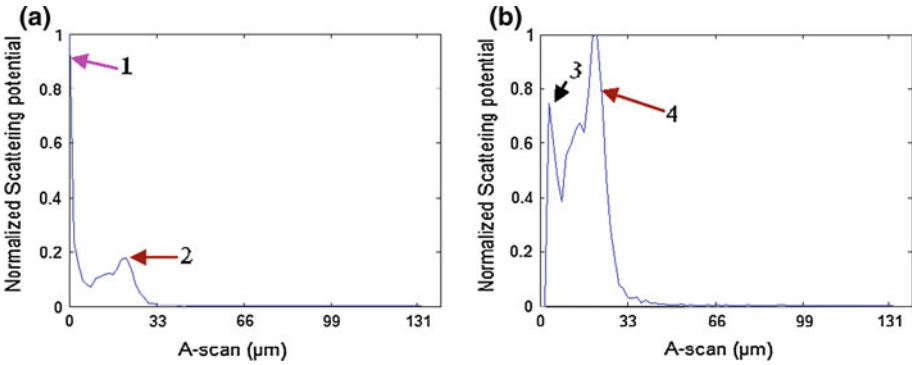

Fig. 4 One-dimensional A-scan image of the sample **a** before and **b** after normalized procedure and the Gaussian spectrum procedure

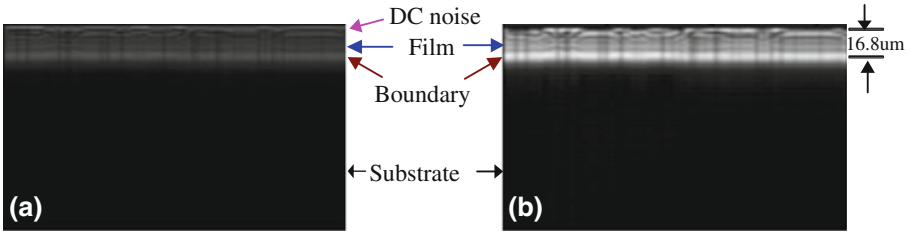

Fig. 5 Two-dimensional cross-sectional image of the single-film sample **a** before and **b** after normalized procedure and the Gaussian spectrum procedure

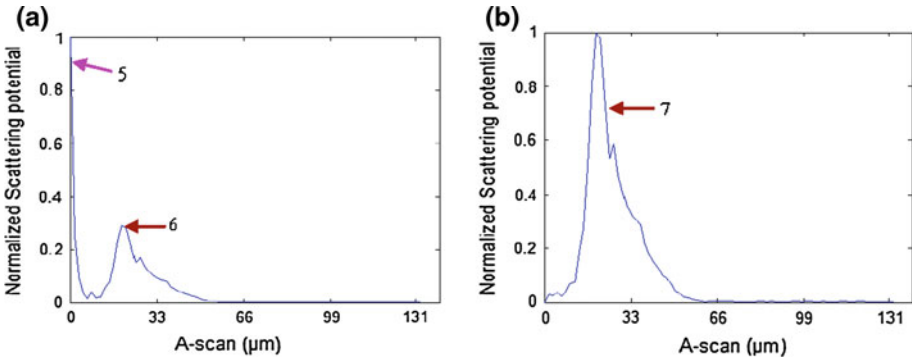

Fig. 6 Two-dimensional cross-sectional Image of the mirror **a** before and **b** after normalized procedure and the Gaussian spectrum procedure

procedure and the Gaussian spectrum procedure, the image is obscure as is shown in Fig. 5a. The image contrast and clarity is low and the microstructure of the sample is difficult to see from the image, therefore, the film thickness is difficult to determine. After the procedures, the image quality is greatly improved, the inner microstructure of the sample can be clear seen as is shown in Fig. 5b, therefore, the boundary is easy to determine. The film thickness measured by this system is 16.8 μm.

Figure 6 shows the one-dimensional normalized scattering potential of the mirror. Scattering potential Peak 5 represents the DC noise of the scattering potential. Scattering potential

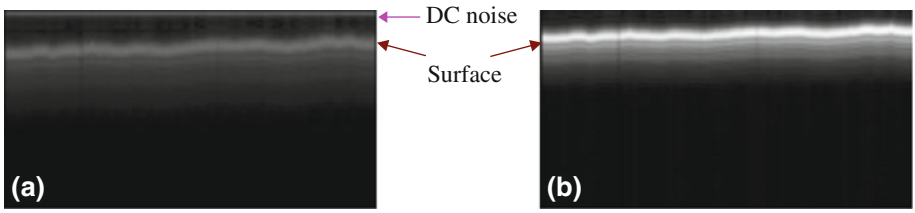

Fig. 7 Two-dimensional cross-sectional image of the mirror **a** before and **b** after normalized procedure and the Gaussian spectrum procedure

Peak 6 and 7 represent the surface of the mirror before and after the normalized procedure respectively. Before the procedures, Peak 6 is small as is shown in Fig. 6a. After the two procedures, peak 7 is sharper than peak 6, and the DC noise (Peak 5) is removed successfully.

Figure 7 shows the two-dimensional cross-sectional image of the mirror. We can see original two-dimensional cross-sectional image of the mirror is obscure, and the image contrast and clarity is low caused by the DC noise and the background noise. After the normalized procedure, the DC noise is removed and the image quality is greatly improved. The microstructure of the mirror became clear as is shown in Fig. 7b.

4 Discussion

The experimental result demonstrates that tungsten halogen light source is suitable for SD-OCT system to achieve ultra-high resolution imaging with high acquisition speed and high image quality. The actual axial resolution of the SD-OCT system in the experiment was $1.2\,\mu$m which was worse than theoretical axial resolution. The calibration error of the frequency linearity may account for the degradation of the axial resolution. The decrease of the scattering potential along axial direction is caused by the decrease of the scattering light intensity because the scattering light becomes weak with the increase of the axial depth in the inner of the sample. After the normalized procedure and the Gaussian spectrum procedure, the image quality was greatly improved and the two-dimensional cross-sectional images became much clearer than before. From the cross-sectional images, we can see the microstructure of the two samples easily. The film thickness of the single-film sample is obtained with this technique although the surface of the film was not absolutely smooth caused by the defective film-coating technology, or the scratches existing in the film. The surface of the mirror is not smooth caused by the defective vacuum coating technology. The slight black lines along vertical direction in the cross-sectional image of the film sample might be caused by the system noises including the optical element stain and the movement of the motion table in the transversal scanning procedure.

5 Conclusion

We have demonstrated a SD-OCT system with a thermal light source applied as low–coherence light source. A simple and effective method without additional equipment was used to remove the DC noise and the background noise of the interference spectrum intensity successfully. With this technique, we obtain two-dimensional (2D) cross-sectional image and the thickness of the single-film. The experiment demonstrates that the proposed normalized

procedure and Gaussian spectral calibration are feasibility to improve the axial resolution and image quality in SD-OCT system. This technique is also helpful to reduce the image acquisition time.

Acknowledgments This work was supported by the National Natural Science Foundation of China (50975228) and the Fundamental Research Funds for the Central Universities.

References

Anna, T., Shaker, C., Mehta, D.S.: Simultaneous tomography and topography of silicon integrated circuits using full-field swept-source optical coherence tomography. J. Opt. A Pure Appl. Opt. **11**, 1–10 (2009)

Brezinski, M.E., Fujimoto, J.G.: Optical coherence tomography: high-resolution imaging in non transparent tissue. IEEE J. Sel. Top. Quantum Electron. **5**(4), 1185–1192 (1999)

Bouma, B.E., Tearney, G.J. et al.: Handbook of Optical coherence tomography. Marcel Dekker, New York (2002)

Chang, S.D., Sherif, S., Mao, Y.X., Flueraru, C.: Swept-source full-field optical coherence microscopy. Proc. SPIE **7386**, 738604-1–6 (2009)

Chen, Y.P., Zhao, H., Wang, Z.: Investigation on spectral-domain optical coherence tomography using a tungsten halogen lamp as light source. Opt. Rev. **16**(1), 26–29 (2009)

Choma, M.A., Sarunic, M.V., Yang, C.H., Izatt, J.A.: Sensitivity advantage of swept source and Fourier domain optical coherence tomography. Opt. Exp. **11**(18), 2184–2189 (2003)

De Boer, J., Cense, B., Park, B.H., Pierce, M.C., Tearney, G.J., Bouma, B.E.: Improved signal-to-noise ratio in spectral-domain compared with time-domain optical coherence tomography. Opt. Lett. **28**(21), 2067–2069 (2003)

Drexler, W., Fujimoto, J.G.: Optical Coherence Tomography. Springer, Berlin (2008)

Dubey, S.K., Anna, T., Shakher, C., Mehta, D.S.: Fingerprint detection using full-field swept-source optical coherence tomography. Appl. Phys. Lett. **91**(18), 181106-1–3 (2007)

Dubey, S.K., Sheoran, G., Anna, T, Anand, A., Mehta, D.S., Shakher, C.: Full-field swept-source optical coherence tomography with Gaussian spectral shaping. Proc. SPIE **7155**, 71551F-1–8 (2008)

Fercher, A.F.: Ophthalmic interferometry: optics in medicine, biology, and environmental research. In: Proceedings of the International Conference on Optics Within Life Sciences (OWLS I), Garmisch-Partenkirchen, Germany, 12–16 August, pp. 221–228 (1990)

Fercher, A.F., Hitzenberger, C.K., Kamp, G., EL-Ziat, S.Y.: Measurement of intraocular distances by backscattering spectral interferometry. Opt. Commun. **117**, 43–48 (1995)

Fercher, A.F., Hitzenberger, C.K., Sticker, M., Barriuso-M, E., Leitgeb, R., Drexler, W., Sattmann, H.: A thermal light source technique for optical coherence tomography. Opt. Commun. **185**, 57–64 (2000)

Fercher, A.F., Drexler, W., Hitzenberger, C.K., Lasser, T.: Optical coherence tomography-principles and applications. Rep. Prog. Phys. **66**, 239–303 (2003)

Huang, D., Swanson, E.A., Lin, J.S.S.C.P., Stinson, W.G., Chang, W., Hee, M.R., Flotte, T., Gregory, K., Puliafito, C.A., Fujimoto, J.G.: Optical coherence tomography. Science **254**, 1178–1181 (1991)

Lee, S.W., Kim, B.M.: Line-field optical coherence tomography using frequency-sweeping source. IEEE J. Sel. Top. Quantum Electron. **14**(1), 50–55 (2008)

Targowski, P., Wojtkowski, M., Kowalczyk, A., Bajraszewski, T., Szkulmowski, M., Gorczynska, I.: Complex spectral OCT in human eye imaging in vivo. Proc. SPIE **5140**, 28–32 (2003)

Tsai, M.T., Lee, H.C., Lu, C.W., Wang, Y.M., Lee, C.K., Yang, C.C., Chiang, C.P.: Delineation of an oral cancer lesion with swept-source optical coherence tomography. J. Biomed. Opt. **13**(4), 044012-1–6 (2008)

Wojtkowski, M., Leitgeb, R., Kowalczyk, A., Bajraszewski, T., Fercher, A.F.: In vivo human retinal imaging by Fourier domain optical coherence tomography. J. Biomed. Opt. **7**(3), 457–463 (2002)

Wojtkowski, M., Srinivasan, V.J., Ko, T.H., Fujimoto, J.G., Kowalczyk, A., Duker, J.S.: Ultrahigh-resolution, high-speed, Fourier domain optical coherence tomography and methods for dispersion compensation. Opt. Exp. **12**(11), 2404–2422 (2004)

Yun, S.H., Tearney, G.J., de Boer, J.F., Bouma, B.E.: High-speed optical frequency-domain imaging. Opt. Exp. **11**(22), 2953–2963 (2003)